Available online at www.sciencedirect.com
SCIENCE DIRECT®
Pergamon
Acta Materialia 51 (2003) 177–193
Acta MATERIALIA
www.actamat-journals.com

Inverse analysis for transient moisture diffusion through fiber-reinforced composites

Pavankiran Vaddadi, Toshio Nakamura *, Raman P. Singh

Department of Mechanical Engineering, State University of New York at Stony Brook, NY 11794, USA

Received 11 February 2002; received in revised form 6 August 2002; accepted 6 August 2002

Abstract

A new approach has been developed, based on an inverse analysis technique, to determine critical moisture diffusion parameters for a fiber-reinforced composite. This technique incorporates two distinct features: direct experimental observations of the weight gained by a composite material exposed to a humid environment, and highly detailed computational analyses that capture the actual heterogeneous microstructure of the composite. The latter feature was carried out by modeling more than 1000 individual carbon fibers that are randomly distributed within an epoxy matrix. The verification and efficacy of this technique was established by conducting an experiment on a high-grade IM7/997 carbon fiber-reinforced epoxy to determine the maximum moisture content at saturation and the diffusivity of epoxy. With the inverse analysis, the time duration required to estimate these moisture diffusion parameters could be drastically reduced as compared to conventional procedures. Subsequently, the established models were employed to characterize transient moisture absorption process within the composite. Here, it was demonstrated that modeling the heterogeneous microstructure of the composite is critical for obtaining accurate diffusion parameters, and an analytical model with effective properties does not produce correct transient moisture absorption behavior. Furthermore, the evolution of stress fields due to moisture induced volumetric expansion was quantified. It was observed that high stress concentrations develop in regions of fiber concentration. These regions then act as potential failure initiation sites that can lead to lower damage tolerance.

Keywords: Carbon fiber-reinforced epoxy; Moisture diffusion; Diffusivity; Maximum moisture content; Inverse analysis; Kalman filter; Randomly distributed fibers

1. Introduction

Fibrous composites, especially carbon fiber-reinforced epoxy are increasingly being used in military and aerospace applications owing to several desirable properties including high specific strength, high specific stiffness and controlled anisotropy. Despite these advantages over conventional structural materials such as metals, composites are susceptible to heat and moisture when operating in harsh and changing environmental conditions. When exposed to humid environments, carbon–epoxy composites absorb moisture and

* Corresponding author. Tel.: +1-631-632-8312; fax: +1-631-632-854.
E-mail address: toshio.nakamura@sunysb.edu (T. Nakamura).

1359-6454/03/$22.00 © Published by Elsevier Science Ltd on behalf of Acta Materialia Inc.
doi:10.1016/S1359-6454(02)00390-7

undergo dilatational expansion. The presence of moisture and the stresses associated with moisture-induced expansion can result in lowered damage tolerance, with an adverse effect on long-term structural durability.

The amount of moisture absorbed by the epoxy matrix is significantly greater than that by the carbon fibers, which absorb very little or no moisture. This results in a significant mismatch in the moisture induced volumetric expansion between the matrix and the fibers, and thus leads to the evolution of localized stress and strain fields in the composite [1]. Additionally, moisture absorption leads to changes in the thermophysical, mechanical and chemical characteristics of the epoxy matrix by plasticization and hydrolysis [2–4]. These changes in the polymer structure lower both the elastic modulus and the glass transition temperature [2–7]. At the same time, moisture wicking along the fiber–matrix interface degrades the fiber–matrix bond, resulting in loss of microstructural integrity. The net effect of moisture absorption is the deterioration of matrix-dominated properties such as compressive strength, interlaminar shear strength, fatigue resistance and impact tolerance [2,5,6,8,9]. These factors lead to reduced damage tolerance and lack of long-term durability. Fig. 1 shows optical micrographs of fiber-reinforced composite subjected to two types of high humidity environment. In the first case, shown in Fig. 1(a), the composite was exposed to 1000 h of 100% relative humidity, while in the second case, shown in Fig. 1(b), the composite was subjected to 2000 h of cyclic exposure to 100% relative humidity and ultra-violet (UV) radiation. Although the level of degradation due to humidity alone is not obvious, when the humid environmental condition is combined with UV exposure, its detrimental effect on the composite becomes obvious. As shown in Fig. 1(b), significant amount of the epoxy matrix was eroded after repeated exposures to humidity and UV. Such degradation decreases the transverse strength and inter-laminar toughness. In light of these observations, the objective of the current work is to characterize and quantify the moisture diffusion process in a fiber-reinforced composite, evaluate the evolution of stress fields due to moisture induced expansions, and in this manner provide

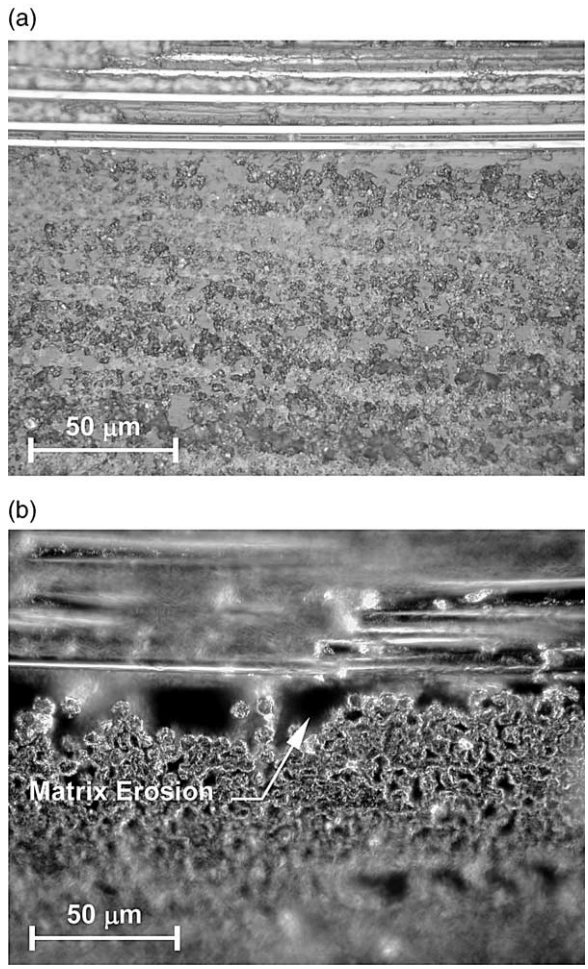

Fig. 1. Optical micrographs of carbon fiber-reinforced epoxy matrix subjected to degradation: (a) 1000 h of exposure to moisture; (b) 2000 h of cyclic exposure to moisture and UV radiation (6 h repeat cycle). In both micrographs, 0° and 90° interlamina interface is shown.

a quantitative basis for predicting the damage tolerance of these materials in humid environments.

Moisture absorption characteristics of composites have been the subject of considerable investigation [10,11] where transient moisture diffusion under normal environmental conditions is approximated as a Fickian process. In homogeneous materials, the kinetics of moisture diffusion is governed by the maximum moisture content and the diffusivity. The maximum moisture content is defined by the net amount of moisture

that a fully saturated material contains under steady state equilibrium when exposed to a given environmental condition. It is usually expressed as the ratio of the increase in weight per unit dry weight at the point of saturation [12]. The time variation of relative weight gain can be measured as,

$$w_t = \frac{W(t) - W_0}{W_0}. \quad (1)$$

Here $W(t)$ is the total weight at time t and W_0 is the reference dry weight of the specimen. The relative weight gain approaches the maximum moisture content of composite at infinite time. It has been shown that the maximum moisture content strongly depends on the relative humidity of the exposure environment [13]. Usually, the maximum moisture content is determined by exposing the material to a humid environment for a long duration of time until steady state equilibrium is attained. This process often takes several months, which makes the procedure cumbersome and time consuming. Also the rate of moisture diffusion is governed by the diffusivity. In general, the diffusivity is a strong function of the ambient temperature and a weak function of the relative humidity.

In the case of composites, the diffusion process is more complex. It depends on the diffusivities of the individual constituents, their relative volume fractions, constituent arrangement and morphology. Traditionally, effective diffusivity has been used to predict the amount of moisture content. The effective diffusivity can be estimated either using a rule-of-mixtures approach or numerical analyses. While the effective or average property is appropriate for conditions under *equilibrium* or *steady-state*, its applicability for transient moisture transport is, at best, questionable. More specifically, under transient condition, the effective or average property may not accurately describe the time variation of moisture content. This aspect has been investigated in detail here. An additional concern with the homogenized rule-of-mixtures approach is that it ignores the microstructural heterogeneity of a fiber-reinforced composite.

This paper presents a novel approach based on an inverse analysis technique to determine the diffusivity and the maximum moisture content for a carbon fiber-reinforced epoxy. First, experiments are conducted to determine the time-variation increase of weight gained by a composite specimen exposed to a humid environment. These measurements are then used as the input into an inverse analysis technique to obtain best estimates of the diffusion parameters. This process also utilizes highly detailed computational analyses of transient moisture transport that account for the actual heterogeneous and complex microstructure of the composite. The net result of this procedure is a complete characterization of the moisture diffusion process.

2. Experimental determination of average weight gain

2.1. Material preparation

Specimens used for experimental determination of average weight gain due to moisture absorption were machined from commercially fabricated $[0]_8$ laminates of IM7/997 carbon fiber-reinforced epoxy donated by Cytec-Fiberite, Inc. The IM7/997 system is currently under development for application to aerospace and rotorcraft structures, and is expected to provide higher damage tolerance than currently qualified materials such as IM7/5271-1 [14]. This composite consists of PAN based, 5 μm diameter, IM7 carbon fibers (Hexcel Composites, Inc.) in a 997 matrix, which is a 177 °C (350 °F) curing, thermoplastic modified, toughened epoxy resin with a proprietary formulation. The average fiber volume fraction for these laminates was determined to be 58% based on microtomography conducted on polished cross-sections shown in Fig. 2.

The specimens were machined using a high-speed diamond saw with water coolant to minimize cutting damage. Specimen edges were then polished to remove microstructural damage that could have been induced during the machining process. In this manner, several specimens were prepared from the $[0]_8$ laminates, with nominal dimensions of 140 × 70 × 1.2 mm. All machined specimens were stored in a desiccator at ambient temperature before testing.

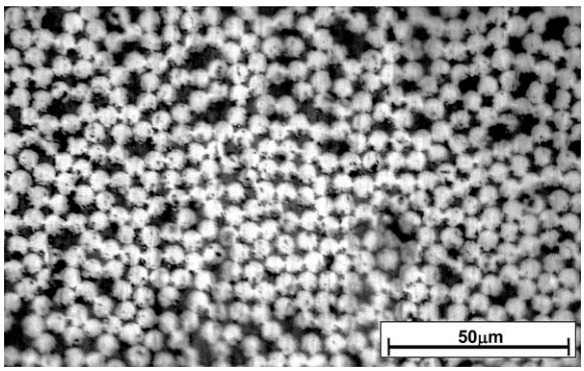

Fig. 2. Cross-section of IM7/997 composites (Cyctec Fiberite, Inc) showing randomly distributed carbon fibers (v_f = 58% and 5 μm diameters) in epoxy matrix.

2.2. Moisture absorption tests

The specimens were preconditioned prior to exposing them to controlled humid environments. This preconditioning procedure involved drying the specimens at 50 °C, until no further change in weight was observed. The procedure normally required 1–2 weeks to remove all residual moisture. Then the reference dry weight, W_0 for each specimen was recorded. Subsequently, these specimens were exposed to various humid environments in a Benchmaster BTRS chamber (Tenney-Lunaire, Inc.). This chamber provides automated cyclic or constant exposure to temperature and humidity for extended durations of time. The objective in these experiments was to determine the average weight gained by a composite specimen, as a function of time, when exposed to given humidity and temperature conditions. The schematic of a thin composite specimen exposed to moisture environment is depicted in Fig. 3.

The specimens were subjected to two distinct environmental conditions in order to establish the validity of the inverse analysis technique for more than one environmental condition. They are: Relative humidity, R_H = 50% and 85% both at T = 85 °C, and R_H = 85% at T = 40 °C. The last condition was tested to investigate the effects of temperature and only the final result is reported here. The exposure temperature, elevated over ambient, was selected to accelerate the moisture transport process. Nevertheless, this temperature

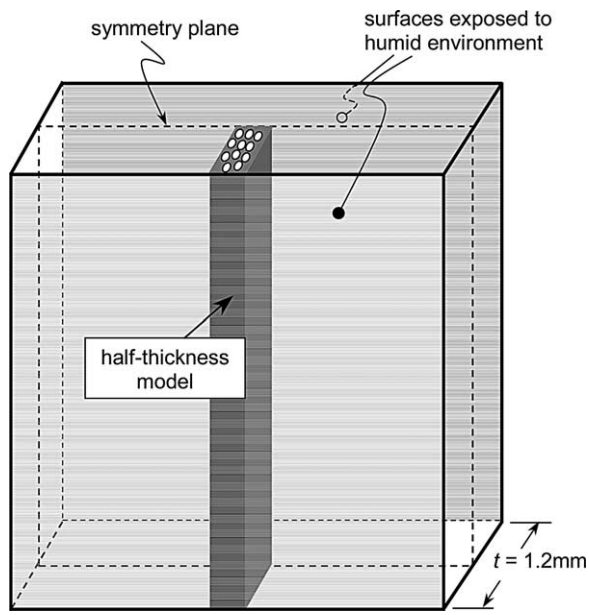

Fig. 3. Thin composite laminate is exposed to humid environment at front and back surfaces. Note the moisture flow from the edges is not considered due to relatively small surface areas. The half-thickness model that is used in the analysis is also illustrated.

was small enough compared to the glass transition temperature of epoxy ($T_g \sim 210$ °C) to safely assume that Fickian moisture diffusion process would not be affected. Two specimens were used for each exposure condition to provide repeatability. Also, fresh, as-received specimens were used for each exposure condition, so that any material changes introduced by moisture cycling would not affect the measurements.

The specimen weight was monitored every 24 h using a high-resolution analytical balance. This balance has a resolution of 0.1mg, which corresponds to monitoring a weight change that is about 5×10^{-4}% of the specimen weight. Based on the periodic weight measurements, the relative weight gain of composite was computed as (1). At every measurement, the specimens were wiped to remove surface condensation. In addition, the weighing process was carried out in a very short time period to minimize the effects of discontinuity in the moisture absorption process. Note that the relative weight gain also represents the relative moisture

content of the whole composite specimen at any given instant of time.

Fig. 4 shows the relative weight gain as a function of time for $[0]_8$ IM7/997 specimens subjected to the two environmental conditions. The experimental data plotted for each case correspond to the average of relative weight gains determined for two specimens. The weight of the specimens increased rapidly during initial periods of exposure for both the environmental conditions. As the specimens were saturated with more moisture, the rate of weight change was lower and the average slope started to approach a value of zero. The relative weight change of the specimens at the end of the exposure duration was higher for $R_H = 85\%$ than that observed for $R_H = 50\%$. This is in accordance with the fact that an exposure environment with higher relative humidity will correspond to a greater value of maximum moisture content, and hence a greater increase in specimen weight. Since the temperature was the same for both environmental conditions, one would expect the diffusivity to be similar and this is reflected by the fact that both curves in Fig. 4 are nearly identical at the initial times. The experimentally determined variation of specimen weight gains were used to estimate the values of the maximum moisture content and diffusivity using an inverse analysis technique, as discussed in the following section.

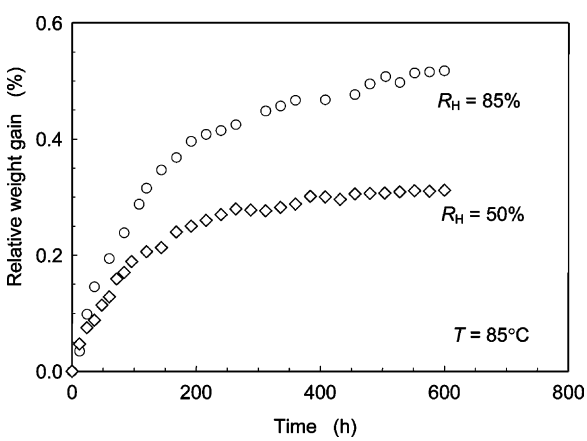

Fig. 4. Measured relative weight gain of composite due to moisture shown as a function of time. Exposed conditions are RH = 50% and 85% both at T = 85 °C. Note that the plot shows the average values from two specimens.

3. Inverse analysis

Inverse analysis is a method by which unknown state parameters are estimated from available data or measurements. It is most effective when direct determination of properties is difficult or impossible, as for complex material systems. In the present analysis, the unknown parameters are chosen as the maximum moisture content, C^*, and the diffusivity, D, of the epoxy matrix. Once C^* is estimated, the maximum moisture content of the composite can be directly obtained from the known matrix weight fraction. For the diffusivity, one may attempt to directly estimate the effective diffusivity of composite by assuming a homogenized property. However, under transient conditions, an estimated moisture absorption determined through such a parameter does not correspond to the actual absorption (discussed in Section 4.3). Therefore it is critical to determine the diffusivity of each constituent in the composite. Since the diffusivity of the carbon fibers is approximated as negligible, only the diffusivity of the epoxy matrix must be determined in this analysis.

Traditionally, maximum moisture content has been determined by monitoring the weight gain of a material that is exposed to a humid environment for a long period of time until steady state equilibrium is attained. Additionally, the direct measurement of diffusivity is very difficult since it is nearly impossible to measure time-variation of point-wise moisture content within the composites. Thus, the inverse analysis technique is ideally suited to make estimations of unknown parameters from limited experimental measurements. Alternatively, the inverse analysis enables estimation of unknown parameters without resorting to complex experimental measurements.

Various optimization and filtering techniques are available to perform inverse analysis. In this investigation, the Kalman filter theory is utilized to estimate the critical moisture transport parameters. This method employs a recursive predictive process and is particularly effective for estimating

unknown variables under nonlinear conditions. Essentially the algorithm updates previous estimates of state parameters through new measurements, and attempts to find the best estimates. Due to its mathematical structure, it has the ability to filter out measurement noise/error and is used in many areas such as sensor calibration, tracking applications, trajectory determination and signal processing [15,16]. The Kalman filter has also been used for the estimation of various unknown material parameters [17–20]. This technique is ideally suited for the present study since the total moisture absorption is nonlinear with time and the weight measurements can contain some errors.

3.1. Kalman filter for transient moisture diffusion

In the Kalman filter, the unknown state parameters are defined as the maximum moisture content of the epoxy, C^*, and the diffusivity of the epoxy, D. The unknown state/material parameters can be expressed in a vector form as $m = (C*, D)^T$. Since the Kalman filter makes successive estimates during $0 < t \leq t_{max}$, we may define the current estimates of the state parameters at time t as $m_t = (C_t*, D_t)^T$, where C_t^* and D_t represent the intermediate values of the maximum moisture content and diffusivity. The estimates are indirectly made from the measured relative weight gain, w_t^{meas}. In general, the weight gain measurement contains error/noise as $w_t^{meas} = w_t + w_t^{err}$, where w_t is the real relative weight gain of the composite and w_t^{err} is the measurement noise at time t. It is assumed that the relative weight gain is a function of the state vector $w_t(m)$, i.e., for given values of maximum moisture content and diffusivity, the relative weight gain at time t can be defined.

After initial estimates C_0^* and D_0 are assigned, subsequent estimates are made through the following updating algorithm using measured weight gain at t.

$$m_t = m_{t\text{-}1} + K_t\,[w_t^{\text{meas}} - w_t(m_{t\text{-}1})], \tag{2}$$

where, K_t is the 'Kalman gain matrix' that is multiplied with the difference of the measured and predicted values of the relative weight gain. Essentially, this matrix is used to make improved estimates at each time step. With two state parameters and one measurement, the dimensions of Kalman gain matrix are 2×1. Note, the Kalman filter may process more than two unknown state parameters and more than one measurement parameter. In the latter case, the measurements can be expressed in a vector form. In general, the estimates of unknown parameters improve with greater number of input measurements. The Kalman gain matrix is computed at each time step aswhere

$$\boldsymbol{K_t = P_t w'^T_t R_t^{-1}} \text{where} \quad \boldsymbol{P_t = P_{t-1}} - \boldsymbol{P_{t-1} w'^T_t (w'_t P_{t-1} w'^T_t + R_t)^{-1} w'_t P_{t-1}}. \tag{3}$$

.Here w'_t is a 1×2 matrix that contains the gradients of w_t with respect to the state parameters C^* and D as,

$$w_t'^T = \frac{\partial w_t}{\partial m_t} = \left(\frac{\partial w_t}{\partial C*}, \frac{\partial w_t}{\partial D}\right). \tag{4}$$

In addition, P_t is the 'measurement covariance matrix' related to the range of unknown state parameters at increment t, and R_t is the 'error covariance matrix' related to the size of measurement error. Once the initial values are imposed, P_t is updated every increment, while R_t needs to be prescribed at each increment. However, in many cases, fixed values can be assigned to the components of R_t as long as measurement error bounds do not vary substantially during the duration of measurements. Since the convergence rate can be significantly affected by the values of P_t and R_t, proper assignments for these two matrices are essential to obtain good estimates. After several trials, the initial measurement covariance matrix and the constant error covariance matrix were assigned in this analysis as,

$$\boldsymbol{P}_0 = \begin{bmatrix} (\Delta C^*)^2 & 0 \\ 0 & (\Delta D)^2 \end{bmatrix}, \quad \boldsymbol{R}_t = [(10R)^2], \tag{5}$$

where, ΔC^* and ΔD denote the expected ranges of the maximum moisture content and diffusivity, i.e., $\Delta C^* = C^*_{\max} - C^*_{\min}$ and $\Delta D = D_{\max} - D_{\min}$. While P_0 is diagonal, the procedure results in a filled matrix for P_t during subsequent increments. In the current analysis, the component of error covariance was chosen to be constant throughout

with a value of $(10R)^2$ where R represents the maximum measurement error relating to measured relative weight gain. Based on the experimental measurements as shown in Fig. 4, the non-dimensional R was given a value of 2×10^{-5}. In general, larger value leads to slower convergence while very small value induces instability and result in convergence to incorrect state parameters. The overall Kalman filter procedure is summarized in the flowchart shown in Fig. 5. This algorithm was implemented in a computational code.

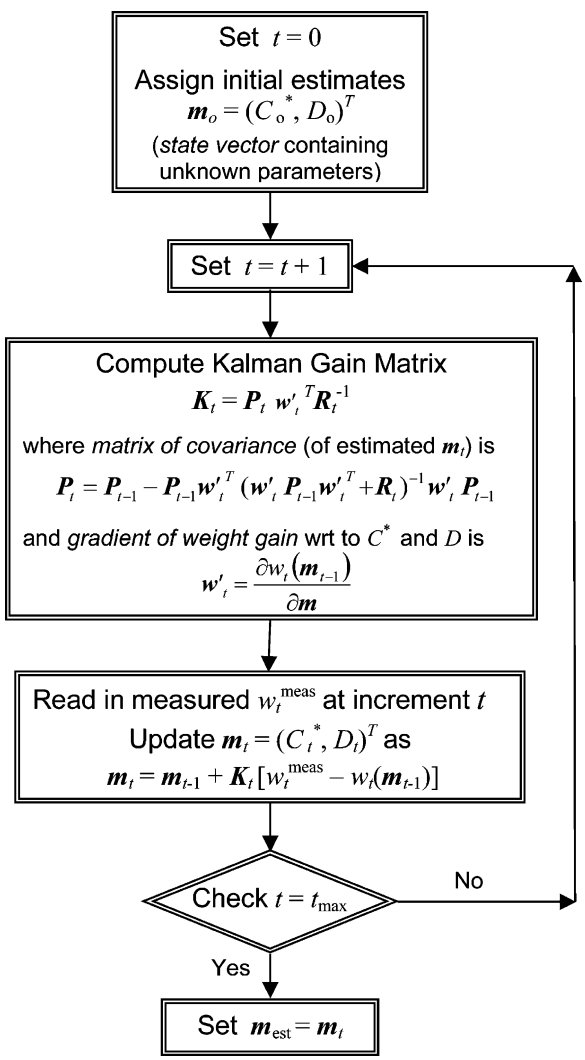

Fig. 5. Flowchart for Kalman filter to estimate the maximum moisture content and the diffusivity from the time-dependent measured weight gain.

As described previously, the Kalman filter requires the relative weight gain w_t and its gradient w'_t for given values of C^* and D to be known a priori. For some simplified problems, these functions may be determined from closed-form analytical solutions. However, in many situations involving complex boundary and geometrical conditions, the solutions can be obtained only through separate numerical analyses. For the case of moisture diffusion, w_t and w'_t can be approximated using the Fickian equation without resorting to detailed computations. Such a procedure, however, was found to be inaccurate for transient moisture transport in fiber-reinforced composites (discussed in Section 4.3). Therefore, detailed finite element models were constructed to simulate moisture absorption process and generate accurate functions for w_t and w'_t, as discussed in the next section.

3.2. Geometrical modeling of composite material

Unlike determination of effective properties of composites under equilibrium and/or steady state conditions where 'unit cell' models are often used, transient analysis requires the modeling of the *entire distance* over which moisture transport occurs. This means one cannot just consider a small region of the specimen to model the transient moisture diffusion behavior. Consider a schematic of the specimen shown in Fig. 3. In the actual experiment, all the surfaces of the specimen are exposed to the humid environment. However, since the total area of the front and back surfaces is much greater than the area of the specimen edges (by a factor of 37), moisture transport across the specimen edges was neglected. This reduces the problem to a two-dimension, which moisture absorption transverse to the fiber direction is considered. In addition, it is necessary to model only half the thickness of the composite specimen, due to the center-plane symmetry condition. For the specific case of carbon fiber-reinforced epoxy, the diffusivity of the carbon fibers is negligible as compared to that of the epoxy matrix. Hence, it is entirely appropriate to consider moisture transport occurring only in the epoxy matrix.

Since the volume fraction and diameter of the carbon fibers is 58% and 5 μm, respectively, and

the specimen half-thickness is 600 μm, about 100 fiber layers can exist from the external surface to the center-plane. Two models were constructed to consider the distribution of the carbon fibers in the epoxy matrix. Initially, the fibers were arranged in a regularly spaced 'hexagonal arrangement'. This required 111 fibers to generate a model that represented the specimen half-thickness, given the fiber volume fraction of 58%. Regularly spaced fiber distributions (e.g., hexagonal packing) have been used successfully in many composite analyses for determining effective material properties. However, it was discovered that they do not capture the moisture transport process of irregularly distributed fibers, as shown in Fig. 2. Therefore, another model was constructed with randomly distributed carbon fibers to capture the nature of actual configuration. The difference in the two models is significant and it will be described in Section 4.2. Due to the inability of hexagonal model to simulate accurate moisture diffusion, the 'random model' was adopted for the inverse analysis. Note that the use of this model requires a more than 50-fold increase in the computational efforts as compared to that of the regular hexagonal model.

In order to model the random fiber arrangements, a computational code was developed to place circular fibers at random positions. Since the specimen has a high fiber volume fraction of 58%, placing every fiber in the domain required special algorithms. In addition, each of the four plies of the specimen half-thickness was modeled separately. This allowed for the incorporation of a thin strip of epoxy rich region along ply interfaces, as shown in Fig. 6. As discussed earlier, the through thickness dimension of the model must equal the half-thickness of the specimen, i.e., 600 μm, but the width of model is limited by computational resources. A greater width results in the modeling of a larger number of fibers, which requires more computation resources. After several trials, the width of the random model was selected to be 64 μm. This dimension allows for 8–10 fibers to be placed across the model width without resulting in prohibitively expensive computations. A total of 1200 fibers were placed in the random fiber model to generate the required fiber volume fraction of 58%, as shown in Fig. 6(a). After establishing the fiber distribution, an automatic mesh generator was used to construct a finite element mesh, shown in Fig. 6(b,c). The element sizes in this mesh were kept sufficiently small for accurate simulation of transient moisture transport. The entire mesh contains more than 130,000 nodes and 240,000 triangular elements. Although detailed convergence analysis was not possible due to its complexity, a separate random mesh was constructed to check for the consistency in the solutions. For uncoupled moisture transport analysis, the elements in the carbon fibers were not included. However, these elements were taken into account for the coupled stress-moisture analysis presented in Section 5.

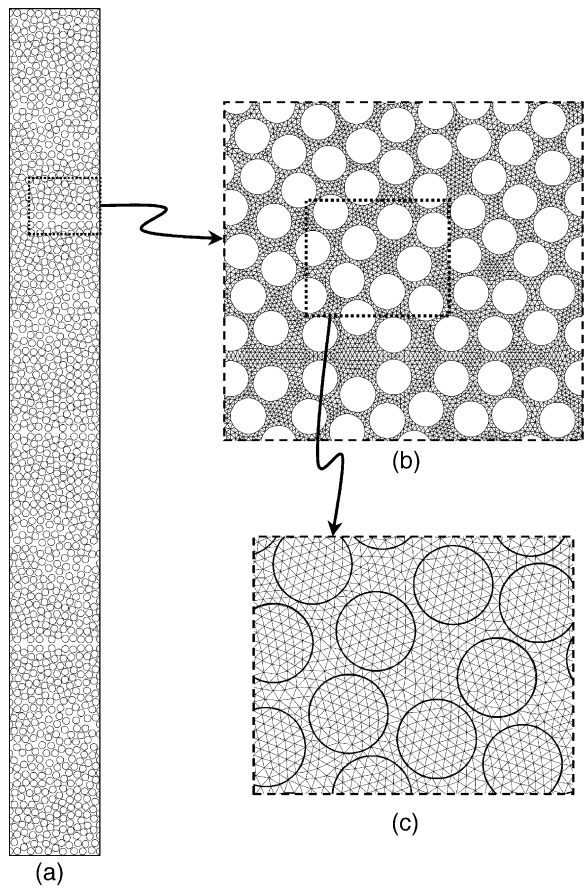

Fig. 6. Schematics of random model used in the transient analysis. (a) Outlines of 1200 fibers are shown in the half-thickness model. (b) Finite element mesh of local region. The elements representing fibers are not shown for clarity. (c) Enlarged view of mesh with fibers.

3.3. Finite element analysis

Finite element analysis was carried out using the finite element code ABAQUS. The analogy between Fick's law for mass diffusion and Fourier's law for heat transfer was employed to model transient moisture diffusion. The mass diffusion coefficient for Fickian diffusion is analogous to the thermal diffusivity coefficient for Fourier heat transfer [21]. In addition, the values of conductivity, specific heat and density, for a heat transfer analysis, can be adjusted appropriately to provide the solution for transient moisture diffusion.

In the moisture diffusion analysis, every node has one degree of freedom and moisture content is directly specified as a nodal value. For the finite element model, moisture transport into the material occurs only across the top surface exposed to the humidity. Thus, it is possible to specify the maximum moisture content for given environmental conditions as the boundary condition on this surface. Symmetry conditions were imposed on all the other three surfaces. At time $t = 0$, the entire specimen had zero moisture content. Many finite element simulations were performed with various values of maximum moisture content and diffusivity of the epoxy. For each case, the computational analysis of moisture diffusion was conducted for more than 600 h in over 100 increments. The total weight gained by the specimen was computed at every 24 h by integrating nodal moisture over the entire epoxy phase in a post-processing program.

3.4. Reference data for weight gain

The inverse analysis requires time-dependent solutions of weight gain for a given set of maximum moisture content and diffusivity of epoxy. This amounts to the determination of the relative weight gain $w_t(C^*, D)$ and its gradients $w'_t(C^*, D)$ as functions of time for various values of C^* and D, which then serve as reference data that are used to update the estimates in the Kalman filter over many time steps. Aforementioned finite element computations were used to establish this reference data. Before developing the complete reference data set, it is important to select the appropriate domain for the unknown state parameters. This ensures that the actual parameters will fall within the selected domain and all estimates will converge to the proper values. The required domain can be estimated either from previous information regarding the unknown state parameters or by running a few trial simulations. A combination of both these approaches was employed to select the domain for the maximum moisture content C^* and the diffusivity D. Here, the reference domain was selected to be $0.57\% \le C^* \le 2.27\%$ and $30 \times 10^{-14}\ \mathrm{m^2/s} \le D \le 75 \times 10^{-14}\ \mathrm{m^2/s}$, respectively. To determine the relative weight gain $w_t(C*, D)$ as a function of time and its gradients $w'_t(C^*, D)$ for any values of C^* and D, the bi-cubic Lagrangian interpolation functions were utilized. The cubic functions ensure interpolated values to be within a few percent of exact solutions. To generate 4×4 base values as shown in Fig. 7, finite element simulations were carried out for 16 different combinations. Values of the relative weight gain at the 16 base points were stored every 24 h and used to determine w_t and w'_t at every Kalman filter increment.

To ensure that the actual values of the unknown

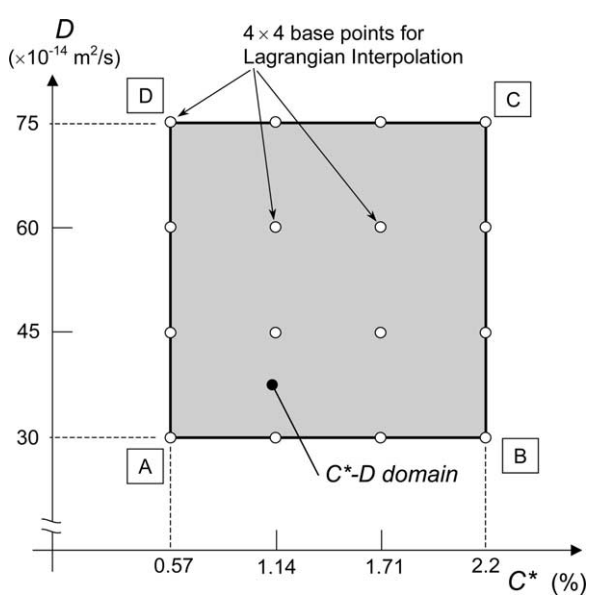

Fig. 7. Domain of unknown state variables (i.e. maximum moisture content and diffusivity) selected to explore their values. The four corner points are denoted as A–D. Bi-cubic Lagrangian functions are used to interpolate values within the domain.

state parameters would fall within this domain, the time-dependent weight gain was computed for four sets of extreme cases of C^* and D, i.e., four combinations of the extreme values. Time variations of the computed weight gain are shown in Fig. 8 along with the experimentally measured data. The fact that the experimental results lie within the extreme cases for entire period is a good indication that the selected domain contains the actual values of the unknown state parameters.

3.5. Estimation of diffusion parameters

The Kalman filter procedure was carried out using the experimentally measured weight gain for two different humidity conditions. In each case, 25 measurements at 24-h intervals (total time of 600 h) were supplied to the inverse analysis to estimate the unknown parameters (i.e., $C*$ and D). At every time increment, the Kalman filter updates the estimate until the last increment is reached. As illustrated in Fig. 5, the Kalman filter requires initial estimates for each process. In general, the final estimates are not identical for different initial estimates and some spread in converged values exists. Since the inverse analysis technique can only provide estimates of the unknown state parameters, there is no unique method to identify the *exact solutions.* However, if the method is robust, the final values corresponding to various initial estimates should converge within small ranges of state parameters.

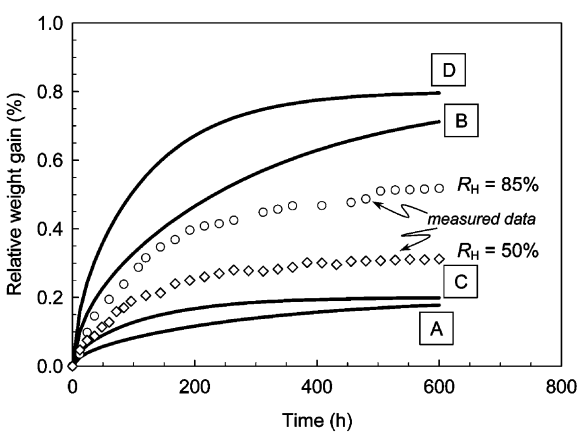

Fig. 8. Increasing relative weight gains computed from the finite element random model. The values of $C*$ and D are chosen at the four corner points A–D shown in Fig. 7. The experimentally measured values fall within these curves.

In the current analysis, an effective approach to obtain the *best estimates* of state variables was established. First, within the predicted domain, $C*$ and D were each incremented into 40 different values. Then the Kalman filter was carried out with 1600 (i.e., 40×40) different initial estimates using the same weight measurement record. The converged locations of all the initial estimates are shown using the intensity of convergence plots in Fig. 9. Essentially, larger contour values signify more initial estimates converged at the particular values of $C*$ and D. The intensity is normalized so that the highest intensity takes the value of 100. Again, a robust process leads to a small region of convergence while ill-conditioned case generates a large or many detached regions of convergence. Generally, a robust process with good convergence characteristics can be attained when the number of measurements is large and the measurements are sensitive to changes in state parameters. Although the present analysis has only one measurement (i.e., weight gain), a relatively good convergence behavior was observed in the both cases. In Fig. 9(a), which represents the convergence plot for $R_H = 50\%$ condition, the two state parameters were estimated as $C^* = 1.03\%$ and $D = 59.2 \times 10^{-14}$ m^2/s, respectively, based on the highest intensity of final convergences. Fig. 9(b) shows the convergence plot for $R_H = 85\%$ condition. It can bee seen the largest intensity occurs near $C^* = 1.48\%$ and $D = 54.4 \times 10^{-14}$ m^2/s. These estimates obtained from the inverse analysis are consistent with known values. As expected, the maximum moisture content is significantly higher under a moister environment (i.e., $R_H = 85\%$). Although the diffusivities are different for the two humidity conditions at the same temperature, they are within 10% of each other. These results confirm that the diffusivity is a weak function of the relative humidity.

Using these best estimates obtained from the inverse analysis as inputs, the moisture diffusion process was re-simulated with the random finite element model. The relative weight gains were

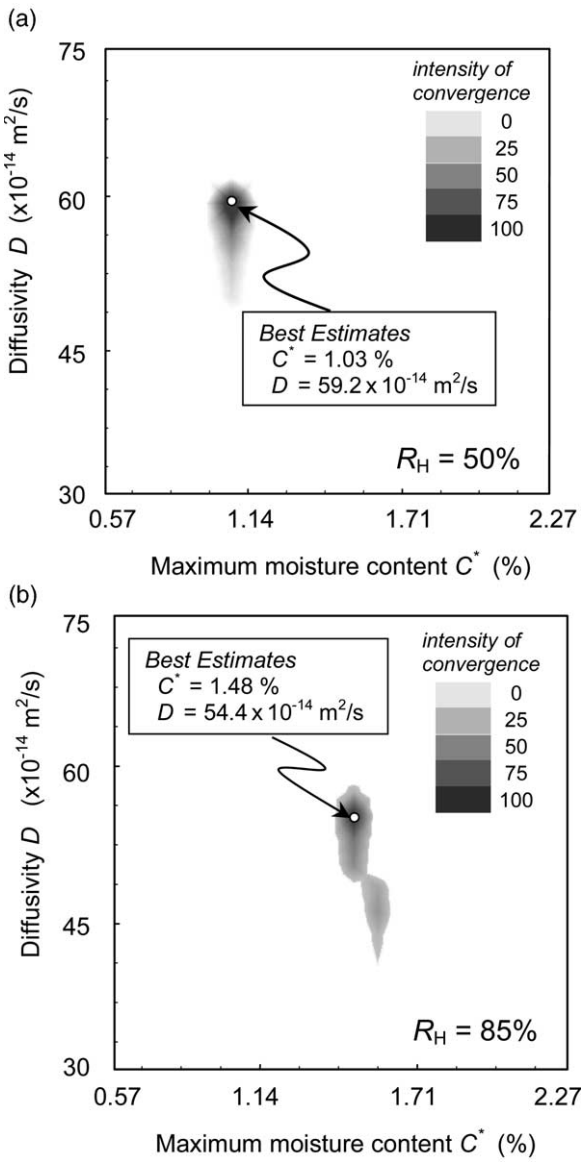

Fig. 9. Inverse analysis generated convergence plot of diffusion parameters for (a) $R_H = 50\%$ and (b) $R_H = 85\%$, both at $T = 85$ °C. A large intensity corresponds to likely convergence of many of initial estimates. In each plot, the location of largest intensity corresponds to the best estimates.

computed and are shown with the measured weight gain for both $R_H = 50\%$ and 85% in Fig. 10. The agreements between the measured and simulated values are remarkable. In both cases, the simulated results remain within the bounds of experimental

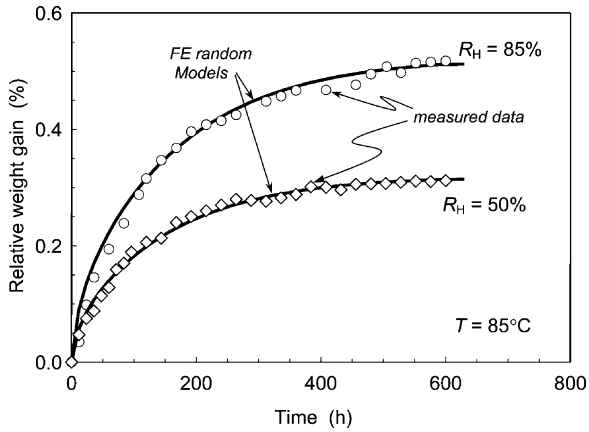

Fig. 10. . Comparisons between experimentally measured and computed weight gains. The latter solutions are obtained from the finite element random models using the best estimates as inputs for the diffusion parameters of epoxy.

error throughout the measured time period ($0 < t < 600$ h). The close match between the simulated results and the experimental observations supports the accuracy of the estimated diffusion parameters determined from the inverse analysis.

We also carried out separate analyses with a reduced measurement period to test if the procedure can still predict accurate values. Using the same measurement record but only up to 312 h, the values of the maximum moisture content and the diffusivity were estimated from similar intensity of convergence plots. Although they are not shown here, the highest converged intensity occurred at $C^* = 1.00\%$ and $D = 63.7 \times 10^{-14}$ m^2/s for $R_H = 50\%$, and $C^* = 1.49\%$ and $D = 54.1 \times 10^{-14}$ m^2/s for $R_H = 85\%$. The two values of maximum moisture content are almost identical to those obtained with the full 600 h measurements. The diffusivity also differs only by 7.6% and 0.6% for $R_H = 50\%$ and 85%, respectively. The accuracies of these short time measurements suggest that the inverse analysis is effective in estimating the critical moisture parameters without taking experimental measurements for a long time.

A separate experiment was conducted to investigate the effect of temperature on the moisture diffusion parameters. The experimental condition being: $R_H = 85\%$ at $T = 40$ °C. The weight

gain measurements are made for up to 1400 h to accommodate slower moisture diffusion. The experimental results were again used to perform the inverse analysis to estimate the maximum moisture content and the diffusivity under this environmental condition. After similar computational procedures, the unknown parameters were estimated to be $C^* = 1.41\%$ and $D = 15.2 \times 10^{-14}$ m^2/s. As expected, the maximum moisture content was unaffected by the temperature change (nearly same as C^* at $R_H = 85\%$ and $T = 85$ °C condition). However, the moisture diffusion was slowed to 30% of the diffusivity at $T = 85$ °C. Results of experimental measurements and computational simulation with the estimated parameters at the lower temperature are shown in Fig. 11. The results at $T = 85$ °C are also shown for reference. Again an excellent correlation is observed for this condition.

4. Transient moisture diffusion process

4.1. Random model

To further investigate the moisture absorption process within the composite, the transient diffusion process was examined in detail. Fig. 12 illustrates the moisture distribution profiles within the composite as a function of time. The surface is exposed to the humidity of $R_H = 85\%$. The moisture contents of the epoxy phase are shown in various gray-scales for four different exposure duration of 144, 288, 432 and 600 h. At region near the moisture-exposed surface, the moisture content immediately saturated and reached the maximum moisture content of $C^* = 1.48\%$. In fact this was the boundary condition prescribed along the exposed plane. Subsequently, the moisture transported toward the symmetric center-plane as time progressed. This process is illustrated by darkening color of the epoxy phase from left to right in Fig. 12. At $t = 600$ h, almost the entire epoxy was fully saturated except near the center-plane. Thereafter the composite would only absorb a limited amount of moisture and hence only a small additional weight gain would be possible.

It is interesting to note that the moisture does not diffuse uniformly across the width of the composite. Disregarding the fiber phase, one can observe that the moisture content is not constant through the width at a given depth (i.e., along the same horizontal location), especially in the earlier time plots ($t = 144$ and 288 h). This occurs due to the random arrangement of the fibers. Since moisture can only diffuse around the fibers, local arrangement of fibers influences the moisture absorption process. The global effects of fiber arrangement on moisture absorption are presented next.

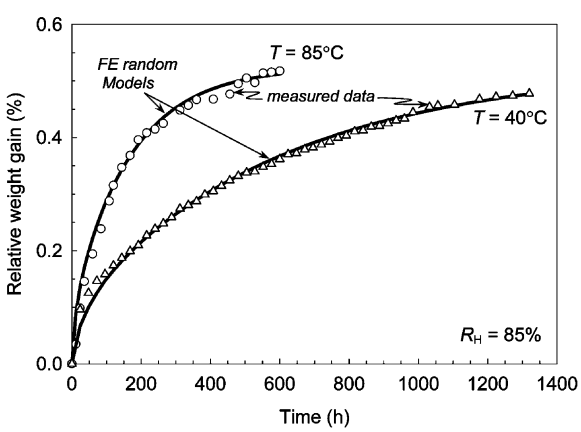

Fig. 11. Effects of temperature are shown for additional test and analysis performed at $T = 40$ °C and $R_H = 85\%$ condition. The results for $T = 85$ °C are also shown for reference. Note that a much longer time is needed to reach the saturation under lower temperature.

4.2. Comparison with hexagonal model

The time-dependent variation of the relative weight gain obtained using the randomly distributed fiber model was compared with that of the hexagonal fiber distribution model. In the hexagonal model, the fibers were arranged regularly to form repeated hexagons. The hexagonal model is often employed in unit cell analyses of fiber or particle-reinforced composites to determine effective material properties. As in the case of random model, the entire half-thickness of the composites containing many fibers were modeled. Though not shown here, a finite element model of a thin strip

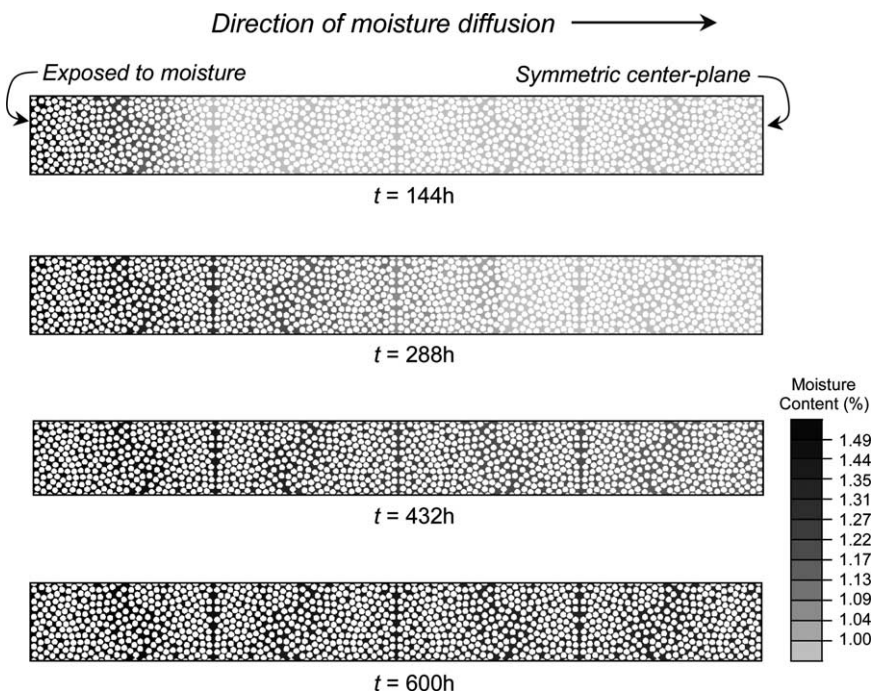

Fig. 12. Shades of transient moisture distribution within epoxy are shown at four different times for $R_H = 85\%$ at $T = 85$ °C. The moisture permeates from the exposed surface on the left to the center-plane of the specimen on the right.

containing 111 half-fibers was constructed for the hexagonal model. The spacing of the fibers is set so that the volume fraction of the fiber is 58% (same as the random model).

The initial and boundary conditions were prescribed identical to those of the random model for $R_H = 85\%$. The computation was carried out for 600+ h and the time variation of the relative weight gain was computed as shown in Fig. 13. The results show sizable difference between the random and hexagonal models. As much as 7% differences were observed between the two models at $t \approx 200$ h. At very long time ($t > 600$ h), both results converged to the same values as the epoxy phase was fully saturated and held the same amount of moisture. The difference at the mid-time period was due to the difference in the moisture flow rate. It is apparent that the effective moisture flow rate or the diffusivity is lower in the random model than that of the hexagonal model. This is attributed to the random fiber model having fiber clustering at many places. This generates more resistance to moisture absorption than the uniformly spaced hexagonal model where moisture transport is easier.

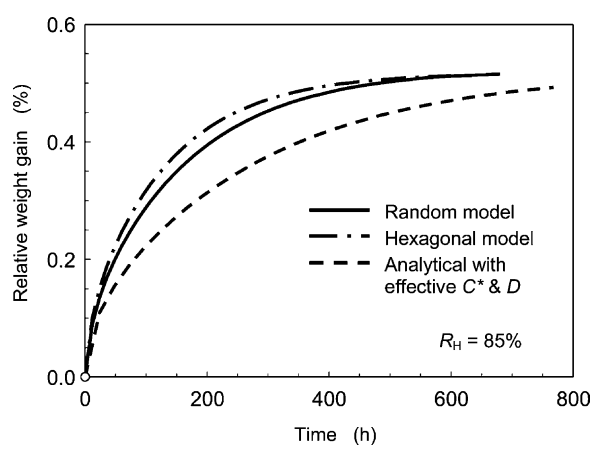

Fig. 13. Comparison between the random hexagonal models for $R_H = 85\%$ at $T = 85$ °C condition. Also the weight gain estimates using the effective properties in the analytical model is shown.

The results shown in Fig. 13 imply that if the hexagonal model were to be used in the inverse

analysis, a different diffusivity for the epoxy would have been estimated. This was the reason for selecting the randomly distributed fiber model in the inverse analysis. For the maximum moisture content, a similar estimate would have been obtained since the saturated weight gain was identical. It is emphasized that the significant difference between the two models arises only under the transient condition. Once the properties of constituents are known, effective properties of composites can be sought in a static or steady-state analysis. In such an analysis, both models yielded nearly identical results. The effective diffusivity of the entire composite was found to be 26% of the epoxy value in both random and hexagonal models.

4.3. Comparison with analytical model

We have also compared the finite element results with analytical solutions. First, the effective diffusivity D_{eff} of the composite was estimated using Halpin–Tsai relation [22,23]. When fibers have circular cross-section and zero diffusivity, the effective diffusivity can be approximated as,

$$D_{\text{eff}} = \frac{1-v_{\text{f}}}{1+v_{\text{f}}}D \tag{6}$$

Here v_{f} is the volume fraction of the fibers and D is the diffusivity of the matrix. With $v_f = 58\%$ in the present composite, Halpin–Tsai model gives $D_{eff} = 0.266D$. This value was nearly identical to the those obtained from the random and hexagonal models under steady-state condition.

Once the effective diffusivity is found and homogenized properties are assumed in the composite, the transient moisture diffusion can be determined from the 1D Fickian diffusion equation shown below.

$$\frac{\partial C}{\partial t} = D_{\text{eff}}\frac{\partial^2 C}{\partial x^2}, \tag{7}$$

where $C = C(x, t)$ is the moisture content and x is the spatial coordinate. Given initial and boundary conditions, the average moisture content can be computed as [10],

$$C_{\text{ave}}(t) = G[(1-\omega_f)C* - C_0] + C_0 \tag{8}$$

where ω_{f} is the weight fraction of the fiber, C_0 is the initial moisture content and C^* is the maximum moisture content of the epoxy and the time dependent parameter $G(t)$ is,

$$G(t) = 1-\frac{8}{\pi^2}\sum_{j=0}^{\infty}\frac{1}{(2j+1)^2}\exp\left[-(2j+1)^2\pi^2\left(\frac{D_{\text{eff}}t}{s^2}\right)\right]. \tag{9}$$

Here s is the thickness of the composite exposed to the humid environment on both sides. Using the above equations with $v_f = 0.35$, $C_0 = 0$, $C^* = 1.48\%$, $D_{eff} = 0.266$, $D = 14.5 \times 10^{-14}$ m^2/s and s = 1.2 mm, one can compute the time variation of the relative weight gain according to the analytical model for $R_H = 85\%$ condition. The result is shown in Fig. 13 along with the computational models. The analytical model exhibited a much lower rate of weight gain as compared to the random model although it approached the same limiting weight gain as the same maximum moisture content was prescribed. The significant difference arises because actual moisture transport rate through the epoxy phase during transient state is higher than the reduced diffusivity represented by the effective value. This results in greater overall moisture absorption rate in the actual heterogeneous model than that of the homogenized model. Based on this observation, it can be concluded that 1D Fickian solution with the effective diffusivity does not properly model the moisture diffusion process in the composite. Furthermore the random fiber distribution model is essential in capturing the features of transient moisture transport in this heterogeneous material.

5. Coupled transient stress and diffusion analysis

The absorption of moisture by carbon–epoxy composites results in the development of stress fields associated with moisture-induced expansion. The constitutive relationship in case of the coupled transient stress and diffusion is an extended form of Hooke's law as

$$\sigma_{ij} = \lambda\varepsilon_{kk}\delta_{ij} + 2\mu\varepsilon_{ij} - (3\lambda + 2\mu)\beta\Delta C\delta_{ij}, \tag{10}$$

where λ and μ are Lame constants, ΔC is the net moisture gain, β is the coefficient of moisture expansion, taken to be 3.24×10^{-3}/ wt.% of water for the epoxy [24] and zero for the fiber. The input values of other material properties are listed in Table 1. Using the random model, coupled transient stress and moisture diffusion analyses were performed to study the internal stress evolution. Here the elements representing the fibers were included in the model. In addition, generalized plane strain elements were employed to allow for out-of-plane deformation. For the displacement boundary condition, symmetry conditions were imposed along the sides of model except along the exposed surface. Essentially the three sides were kept straight and the four corners were set to remain perpendicular. The moisture condition follows that of $R_H = 85\%$.

Fig. 14 shows the von Mises stress distributions in the epoxy matrix at four different local regions at $t = 432$ h. The moisture content at this time is shown in Fig. 12. Although the stresses within the fibers are not zero, they are not shown for clarity. Within the epoxy the normal stresses are generally in compression but their magnitude can reach as much as 30 MPa. This magnitude is significant for epoxy. Furthermore, it can be observed that the stress levels are generally higher within the moisture rich regions (i.e., location A) than those in the less moist region (i.e., location D). Within each region, the stress magnitude varies significantly. For example, within location B, the lowest von Mises stress is about 6 MPa while the highest reaches 30 MPa. Large stresses appear in the region between neighboring fibers. In fact, they are larger where separation distances between fibers are smaller. Although not shown here, when the moisture content reaches the full saturation ($t \approx 600$ h), the levels of stress distributions at the four locations (A–D) become very similar.

Table 1
Mechanical properties of IM7 carbon fiber and 997 epoxy

Property	IM7 fiber	997 epoxy
Young's modulus (GPa)	20 (transverse)	4.14
Poisson's ratio	0.33	0.36
Tensile strength (MPa)	5150	90
Density (kg/m^3)	1780	1310

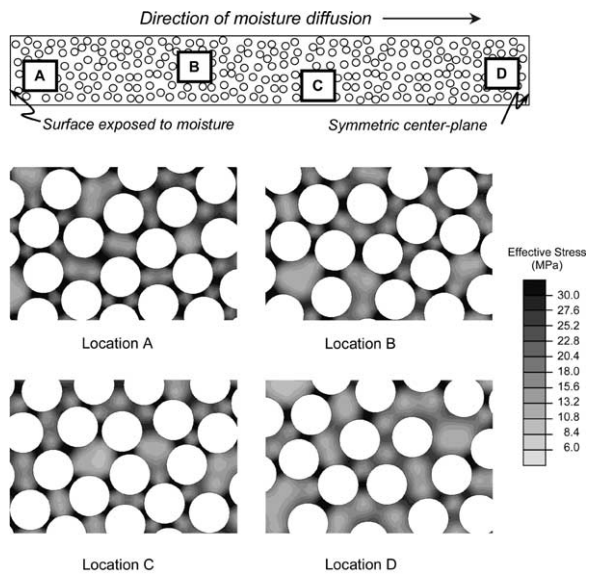

Fig. 14. Shades of Mises stress in the epoxy at $t = 432$ h for $R_H = 85\%$ at $T = 85$ °C. They are shown at four different local locations through-thickness as indicated in the top schematic. Stresses within carbon fibers are not shown for clarity.

6. Discussions

A new procedure based on inverse analysis and simple weight measurements is presented to estimate critical moisture diffusion parameters of composite. The procedure was tested with actual high-grade carbon–epoxy composite specimens placed in a controlled environmental chamber. Using the measured relative weight gain as input, the inverse analysis technique was utilized to obtain *best estimates* of the diffusivity and the maximum moisture content of the epoxy phase. The inverse analysis uses Kalman filter, which is well suited for estimating unknown state parameters under non-linear transient conditions. In order to reference the measured weight gain with the diffusion parameters, a detailed finite element model was constructed. The half-thickness composite model contained well over 1000 individual fibers, and they were distributed randomly so that it captured the key geometrical feature of real composites. From the compari-

son study with a simpler model (i.e., hexagonal model) and analytical approximation, we found that modeling of many randomly distributed fibers was critical for obtaining accurate estimates of moisture diffusion parameters.

Our study also quantifies the differences in transient moisture absorption between the heterogeneous model and the analytical model with effective properties. Large differences indicate that the determination of each constituent's diffusion parameters is critical. Instead of determining the diffusivity and maximum moisture content of epoxy already in the composite, one may opt to seek these parameters for bulk epoxy. However, in many instances, the same particular epoxy is not available in bulk form, and the curing process used for composites may not produce same diffusion properties for epoxy. Furthermore, the present procedure also allows for the testing of aged composites to determine their moisture transport characteristics.

In general, to achieve good convergence characteristics in the inverse analysis, measurement of more than one single parameter is needed. However, to keep the experiment simple and to avoid additional measurements for the moisture absorption, a potential convergence problem was overcome by supplying the weight gain measurement at many time increments (i.e., every 24 h) in the present inverse analysis. Although true values of the unknown parameters cannot be verified in any inverse analyses, the best estimates for the diffusivity and the maximum moisture content obtained here showed high degree of accuracy. The simulated results, using the best estimates as input, produced an extremely good correlation with the experimentally measured record. The utilization of inverse analysis allows not only the effective use of the experimental measurements but also shortens the measurement duration drastically. Our results also show that good estimates can be obtained with a fraction of time needed to reach full moisture saturation of the composite. This feature is particularly attractive for testing at lower temperatures when saturation may take several months, if not years. The required steps in the proposed procedure to measure the diffusivity and the maximum moisture content are summarized below.

1. Carry out moisture absorption test for specific environmental conditions and measure the weight gain periodically (e.g., every 24 h).
2. Perform preliminary finite element analysis and compare the results with the experimental record to ensure the selected domain of unknown parameters is appropriate.
3. Establish reference data for the inverse analysis by generating the weight gains for various sets of state parameters (C^*, D). Use cubic Lagrangian functions to interpolate the relative weight gain and its gradient with respect to the state parameters.
4. Prescribe suitable values for co-variant matrices P_0 and R_t.
5. Carry out the Kalman filter process for various sets of initial estimates for C^* and D. Create intensity of convergence plots to determine the best estimates.

A separate study from the coupled stress-moisture flow analysis revealed high stress concentration near regions of fiber clustering during moisture absorption. The magnitudes of stresses can reach significant level and these regions would be susceptible to damage initiation. Although residual stresses generated during manufacturing as well as the mismatch in the coefficients of thermal expansion were not accounted in the present study, these effects will be included in a future analysis.

7. Acknowledgments

We gratefully acknowledge the US Army Research Office for supporting this research under grant no. DAAD19-00-1-0518. We are also thankful to Mr. J. Morris and Mr. S. Fattohi of Cytec-Fiberite Inc., Anaheim, CA for donating IM7/997 composite laminates used in this project.

References

[1] Lee MC, Peppas NA. Journal of Composite Materials 1993;27(12):1146.
[2] Weitsman YJ. Fatigue of composite materials. New York: Elsevier, 1991.

[3] Jones FR. Reinforced plastics durability. Cambridge, UK: Woodhead Publishing Company, 1999.
[4] Zheng Q, Morgan RJ. Journal of Composite Materials 1993;27(15):1465.
[5] Adams RD, Singh MM. Composites Science and Technology 1996;56(8):977.
[6] Zhao SX, Gaedke M. Advanced Composites Materials 1996;5(4):291.
[7] Choi HS, Ahn KJ, Nam JD, Chun HJ. Composites Part A: Applied Science and Manufacturing 2001;32(5):709.
[8] Soutis C, Turkmen D. Journal of Composite Materials 1997;31(8):832.
[9] Sala G. Composites Part B-Engineering 2000;31(5):357.
[10] Shen CH, Springer GS. Environmental effects on composite materials. Lancaster, PA: Technomic, 1981.
[11] Browning CE, Husman GE, Whitney JMC. In: Composite materials: testing and design, ASTM STP 617. Philadelphia, PA: American Society for Testing and Materials; 1977. p. 48-1.
[12] ASTM D5229/D 5229M Standard test method for moisture absorption properties and equilibrium conditioning of polymer matrix composite materials. American Society for Testing and Materials, Philadelphia, PA; 1992, p. 481.
[13] Loos AC, Springer GS. Journal of Composite Materials 1979;13:131.
[14] Morris J. Private communication. Cytec-Fiberite, Inc., Anaheim, CA; 2001.
[15] Kalman RE. ASME Journal of Basic Engineering 1960;82D:35.
[16] Grewal MS, Andrews AP. Kalman filtering: theory and practice. Englewood Cliffs, NJ: Prentice-Hall, 1993.
[17] Hoshiya M, Saito E. Journal of Engineering Mechanics 1984;110:1757.
[18] Ishida R. Transactions of Japanese Society of Mechanical Engineers Part A 1994;60:443.
[19] Aoki S, Amaya K, Sahashi M, Nakamura T. Computational Mechanics 1997;19:501.
[20] Nakamura T, Sampath S, Wang T. Acta Materialia 4293;2000:48.
[21] Lundgren JE, Gudmundsen P. Composites Science and Technology 1983;1999:59.
[22] Halpin JC. Primer on composite materials: analysis. Lancaster, PA: Technomic, 1984.
[23] Springer GS. Environmental effects on composite materials. Lancaster, PA: Technomic, 1984.
[24] Tsotsis TK, Weitsman Y. Journal of Composite Materials 1990;24:483.